JOURNAL OF MATERIALS SCIENCE 19 (1984) 1242–1250

Reactive processing of titanium carbide with titanium

Part 2 *Solid-state hot pressing*

CANDACE JO QUINN,* DAVID L. KOHLSTEDT
Department of Materials Science and Engineering, Cornell University, Ithaca, NY 14853, USA

The reactive hot pressing of titanium–titanium carbide mixtures to form substoichiometric titanium carbide was studied as a function of time, temperature, pressure and composition using a Box–Behnken experimental design. Thirty samples were hot pressed at 1200 to 1600° C and 7 to 35 MPa (1000 to 5000 psi) for 0.5 to 1.5 h from mixtures containing 10 to 30 vol % titanium metal. Twenty three of these samples had final densities in excess of 95% of the theoretical value. A model for the grain growth during hot pressing was developed by consideration of Kuczynski's semi-empirical sintering model and classical grain-growth models. The modification involves development of a factor which describes the behaviour of the system as a function of composition. Microstructural data, selected area diffraction patterns, and the activation energy for grain growth all indicate that the grain growth is controlled by diffusion through Ti_2C–TiC and/or TiC–TiC boundaries. Densification during hot pressing was interpreted in terms of the creep of titanium metal using a power-law creep model. The activation energy for densification agrees well with the activation energy for the self-diffusion of titanium. The high densities obtained also indicate that the densification depends largely on the ductile nature of the titanium metal.

1. Introduction

The extremely hard, refractory transition-metal carbides are difficult and expensive to process to high density by conventional sintering or hot-pressing techniques. The addition of a low-melting binder phase, such as nickel, cobalt or iron, is a widely used technique for producing high-density, tough cermets for applications such as cutting tools [1]. The use of a base-metal binder circumvents the forming problems common to carbides, but it also limits the upper temperature at which the two-phase cermet can be used.

Titanium carbide, like other transition metal carbides, exists over a wide range of composition, $TiC_{0.97}$ to $TiC_{0.47}$ [2]. This range of composition indicates that mixtures of titanium metal and titanium carbide can be reacted to from substoichiometric titanium carbide. Two properties of titanium metal facilitate the fabrication of high-density substoichiometric titanium carbide via the reaction of titanium carbide with titanium metal. The first of these properties, the relatively low melting point of titanium (1642°C, $\sim 0.5\,T_m$ of TiC), was exploited previously to liquid-phase reaction sinter compacts of titanium carbide plus titanium metal above the eutectic temperature [3]. This process yielded carbides of only modest densities, $< 85\%$ of theoretical. The second property of interest is the ductility of titanium metal. Creep data are available for both titanium [4] and titanium carbide [5] at an applied force of 7000 psi. The creep rate at 1400° C calculated from these data is 7×10^{-4} for titanium metal and 2×10^{-7} for titanium carbide. Reactive hot

*With Corning Glass Works, Ceramic Research Department, Sullivan Park, Corning, NY 14831, USA.

0022–2461/84 $03.00 + .12

TABLE I Reactive hot pressing of titanium–titanium-carbide powders

Sample	Temperature (° C)	Time (h)	Pressure (MPa)	Bulk C–Ti	Grain size (μm)	% open porosity	Density (s cm^{-3})
1	1200	0.5	21	0.69	16.3	8.2	4.66
2	1600	0.5	21	0.69	49.9	0.4	4.63
3	1200	1.5	21	0.69	13.9	10.0	4.68
4	1600	1.5	21	0.69	75.5	2.3	4.75
5	1400	1.0	7	0.75	16.3	14.5	4.67
6	1400	1.0	35	0.75	16.7	3.6	4.73
7	1400	1.0	7	0.63	43.8	1.0	4.60
8	1400	1.0	35	0.63	35.8	0.3	4.74
9	1400	1.0	21	0.69	31.9	0.7*	4.73
10	1400	1.0	21	0.69	58.0	0.6*	4.64
11	1200	1.0	21	0.75	20.0	16.1	4.68
12	1600	1.0	21	0.75	35.2	2.2	4.68
13	1200	1.0	21	0.63	19.6	0.7	4.49
14	1600	1.0	21	0.63	52.1	0.6	4.76
15	1400	0.5	7	0.69	20.8	9.6	4.71
16	1400	1.5	7	0.69	30.6	0.0	4.79
17	1400	0.5	35	0.69	26.3	1.0	4.57
18	1400	1.5	35	0.69	34.1	2.3*	4.95
19	1400	1.0	21	0.69	25.3	1.3*	4.80
20	1400	1.0	21	0.69	21.8	1.3	4.49
21	1400	0.5	21	0.75	18.8	13.8	4.73
22	1400	1.5	21	0.75	19.2	3.5	4.69
23	1400	0.5	21	0.63	35.9	0.4	4.67
24	1400	1.5	21	0.63	33.7	1.6	4.79
25	1200	1.0	7	0.69	14.9	14.2	4.61
26	1600	1.0	7	0.69	44.2	0.6	4.65
27	1200	1.0	35	0.69	18.6	7.1	4.62
28	1600	1.0	35	0.69	48.8	0.7	4.80
29	1400	1.0	21	0.69	35.8	1.2*	4.60
30	1400	1.0	21	0.69	24.5	0.4*	4.70
31	1400	1.0	21	0.94†	14.0	15.0†	4.77

*Replicated midpoint.
†No titanium metal added.

pressing below the liquidus, a process which makes use of the ductility of titanium, is the subject of this paper.

2. Experimental design

The experimental design chosen for the present study was developed by Box and Behnken [6]. The independent variables (those controlled by the experimenter) used in this work were time, temperature, titanium content and pressure. The values of these four variables for the thirty runs reported here are listed in Table I. Fig. 1 is an illustration of the Box–Behnken design in three variables. The Box–Behnken is an efficient design, calling for twenty four runs, plus the centre point, to study four variables at three levels. The experimental points are chosen so that they are each an equal distance from the centre point and therefore lie on the surface of a sphere in the variable space. If the ranges of the independent variables are appropriately chosen, so that each variable has an effect of similar magnitude, the variance is equal in all directions and an unbiased view of the response surface is obtained. Six replicates were run at the centre point.

The hot-pressing data were interpreted in terms of grain growth and densification models adapted from the literature. Modelling was done by a least-squares linear regression. The goodness of fit was judged in terms of the residuals from regression and the square of the multiple correlation coefficient [3].

3. Experimental methods

The titanium and titanium carbide powders were the same as those used in the previously described sintering study [3]. Average particle sizes of 10 and 7 μm, respectively, were measured by Coulter

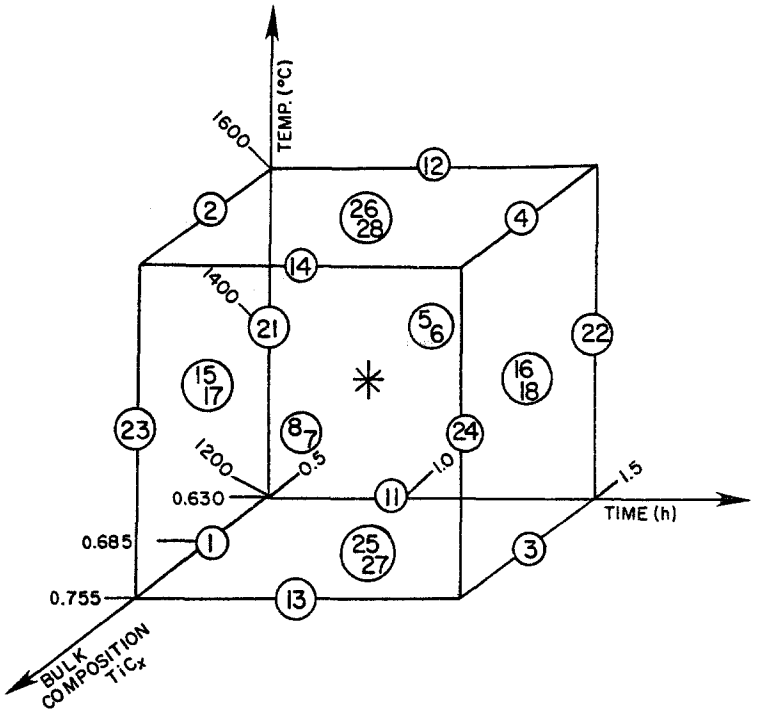

Figure 1 The Box–Behnken experimental design used to investigate the reactive hot pressing of titanium–titanium carbide mixtures. The experiment was run with four variables, time, temperature, composition and pressure, but is condensed here onto three axes. The numbers are the sample identification numbers from Table I.

counter. The carbon and oxygen levels were measured by Leco analysis, and the sample purity was determined by flame emission spectroscopy. Oxygen was a primary contaminant. Some metal contaminants (Fe, Ni and Co) were detected, presumably from milling operations. The carbon–metal ratio, x, of the TiC_x powder was 0.94.

Mixtures of titanium and titanium carbide were prepared in 100 g lots by tumbling in nalgene jars for a minimum of 16 h. The loose powder mixtures were poured into a 5 cm i.d. graphite die which was placed in an induction furnace. The sample was heated under a vacuum of 3×10^{-2} torr using the graphite die as the susceptor. A W/W–26% Re thermocouple placed in the die wall was used to measure the temperature. Pressure was applied hydraulically when the temperature reached 1000° C.

Open porosity and density were determined by Archimedes' principle. The porosity calculated from the measured density as $P = 1 -$ (bulk density/theoretical density) is a function of both composition and degree of reaction. Incompletely reacted samples can exceed the theoretical density of fully reacted material, yet contain some porosity because of the high vacancy concentration on the carbon sublattice in TiC.

X-ray diffractometer traces were obtained on powders prepared from each of the hot-pressed samples to determine the major crystalline phases present. Metallographic samples were prepared and examined as described previously [3]. Portions of mechanically thinned samples were ion-thinned to produce specimens for transmission electron microscopy (TEM) observations which were carried out on a Siemens 102 operating at 125 kV.

4. Results

The crystalline phases, grain size, density and porosity of the hot-pressed samples are tabulated in Table I. Also included in the table is a reference sample of titanium carbide, hot pressed without titanium metal. X-ray diffraction data indicated that TiC is the major crystalline phase in all of the hot-pressed samples. From 2 to 5% residual titanium metal was detected in the high-titanium samples processed at low temperatures and short times. A small (< 2% relative intensity) extra diffraction peak at 0.213 nm was observed on the shoulder of the strong TiC (2 0 0) peak in the hot-pressed samples whose bulk composition was $TiC_{0.63}$ (e.g. those highest in titanium). This peak is from neither TiC nor titanium and is not a strong peak listed for a titanium oxide in the JCPDS file.

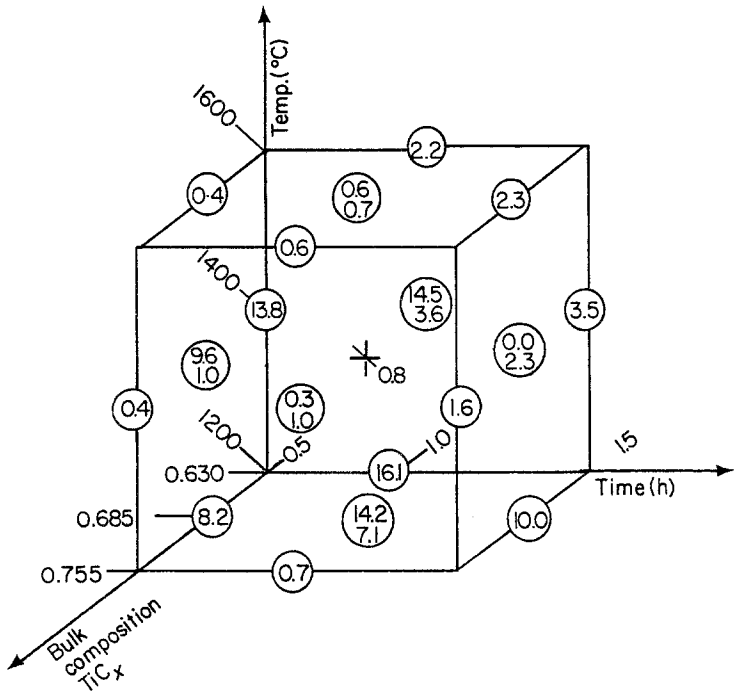

Figure 2 The Box–Behnken experimental design of Fig. 1 is shown with the open porosities of the hot-pressed samples.

The relative densities of the hot-pressed samples ranged from 85% to >99% (the porosity from 15% to <1%). These results are shown in Fig. 2 in relation to the experimental design. The mean grain size is shown in relation to the experimental design in Fig. 3. The average grain sizes of the hot-pressed samples, which ranged from 14 to 65 μm, were measured from optical micrographs such as those in Fig. 4. The intragranular texture in these micrographs suggests the presence of a second phase. This intragranular texture was observed in all samples which exhibited the extra diffraction

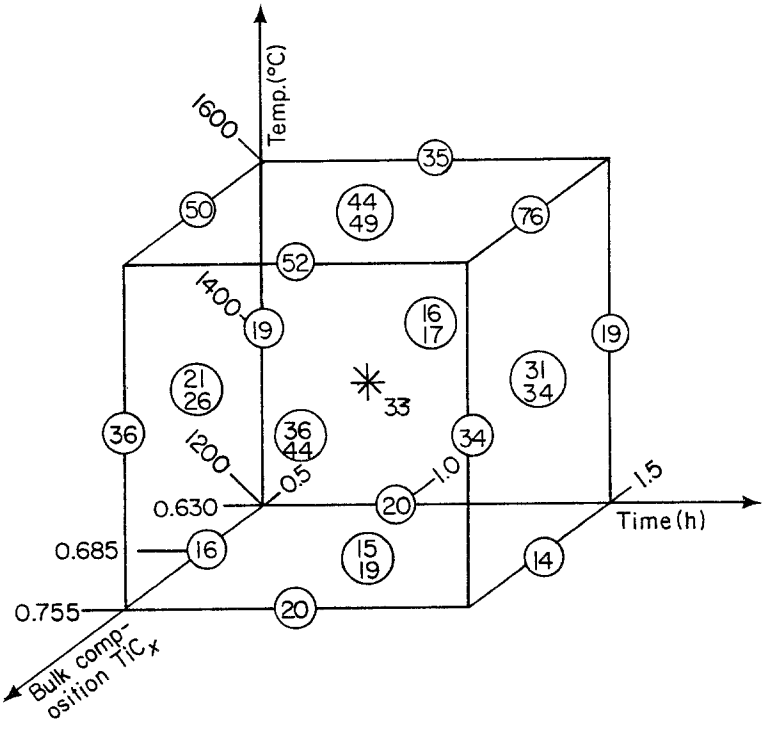

Figure 3 The Box–Behnken experimental design is shown with the mean grain sizes of the hot-pressed samples.

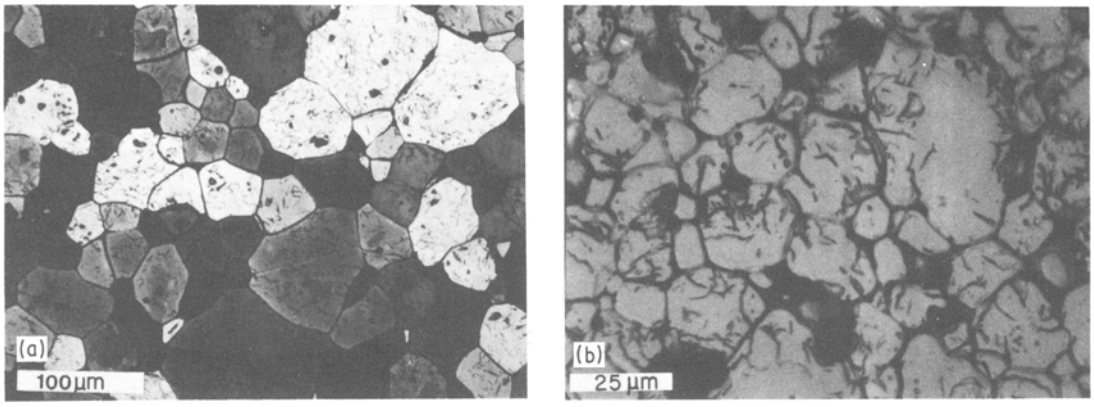

Figure 4 Optical micrographs of hot-pressed Ti + TiC samples. (a) Sample 24 of bulk composition $TiC_{0.63}$ was pressed at 1400° C and 21 MPa for 1.5 h. The section has been polished and etched to reveal an intragranular second phase. (b) Sample 23 was pressed at 1400° C and 21 MPa for 0.5 h. A fine second phase extends from grain boundaries into the carbide grains.

peak at 0.213 nm, although not all samples having an intragranular structure produced a diffraction peak at 0.213 nm.

TEM examination revealed that a second phase does in fact exist in the TiC grains. Figs. 5a to d are TEM micrographs of reaction hot-pressed TiC. Titanium metal is observed in some of the triple junctions (Figs. 5a and b); and a second phase is found as platelets within TiC grains and along grain boundaries (Figs. 5c and d). Selected area diffraction patterns such as Fig. 6 were collected from a number of platelets. These patterns can be indexed on the basis of the orthorhombic Ti_2C unit cell which has recently been discussed for Ti_2C platelets observed in titanium–titanium carbide single-crystal reaction couples [10].

5. Modelling of hot-pressing process

5.1. Densification

The ductile nature of titanium must play an important role in densification, since the densities obtained via hot pressing were considerably better than those obtained by sintering [3]. Several authors (see for example [8]) have described densification during hot pressing by a power-law creep model. The effective stress in such a model is a function of the porosity of the sample and a correction must be made accordingly. One such correction is given in terms of the relative density [9]:

$$\frac{d\rho}{dt} = \frac{A\sigma^p D(1-\rho)}{a_0^r} \qquad (1)$$

where σ is the applied force, D is a diffusion coefficient, t is the time, and a_0 is the initial grain size. Rearranging and substituting for porosity gives:

$$1/P = A_1\sigma^p \exp[-Q/RT]\, tP/a_0^r - 1/P_0. \qquad (1a)$$

In this case, P_0 is the porosity at the time the run temperature is reached. P_0 must be greater than 0.16 since one sample (No. 10) has a final porosity of 16%, and it is probably much larger, say between 0.3 and 0.5. Since the final porosity, P, is less than 0.05 for most of the hot-pressed samples, $1/P$ is substantially greater than $1/P_0$ for most, if not all, of the hot-pressed samples. Thus, we have neglected the $1/P_0$ term in Equation 1a; the application of Equation 1a to the hot pressing data is greatly facilitated by this omission. All of the samples were hot pressed from the same starting powders, so the a_0 term is a constant for these data and $A_1 = A/a_0^r$. The densification of Ti–TiC powders is also a function of composition. By analogy with the reactive sintering model developed previously, we will describe this composition dependence by a power-law function. The equation used to model the densification during hot pressing is then

$$1/P = A_2\sigma^p \exp[-Q/RT] C^q t^s. \qquad (1b)$$

Equation 1b is applied to the hot-pressing data by taking the logarithm of both sides and calculating Q, p, q, and s by least-squares linear regression. One sample, No. 16, had zero open porosity so that $1/P$ is undefined. This sample was excluded in fitting the porosity data to Equation 1b. The result of the regression analysis is

$$1/P = 156\sigma^{0.7} \exp[-117\,\text{kJ}/RT]\, C^{12.7} t^{-0.1} \qquad (1c)$$

with $R^2 = 65.7\%$, corrected for degrees of freedom.

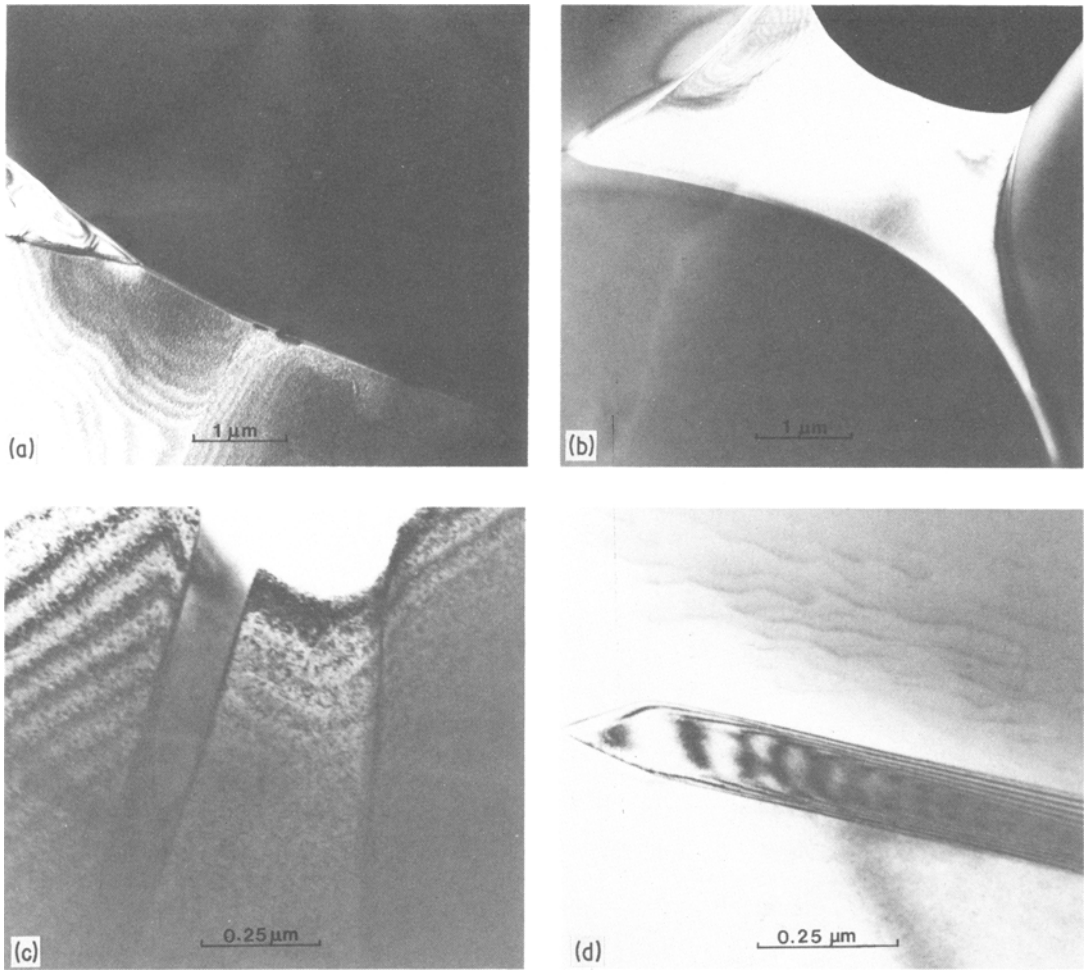

Figure 5 Transmission electron micrographs of reaction-hot-pressed samples. (a) A second-phase particle (WC?) is present in the grain boundary and Ti metal is present in a triple junction of sample 23. (b) This dark-field micrograph sample 23 shows a triple junction containing Ti metal. (c) and (d) These micrographs of sample 14 show Ti_2C platelets in a TiC grain.

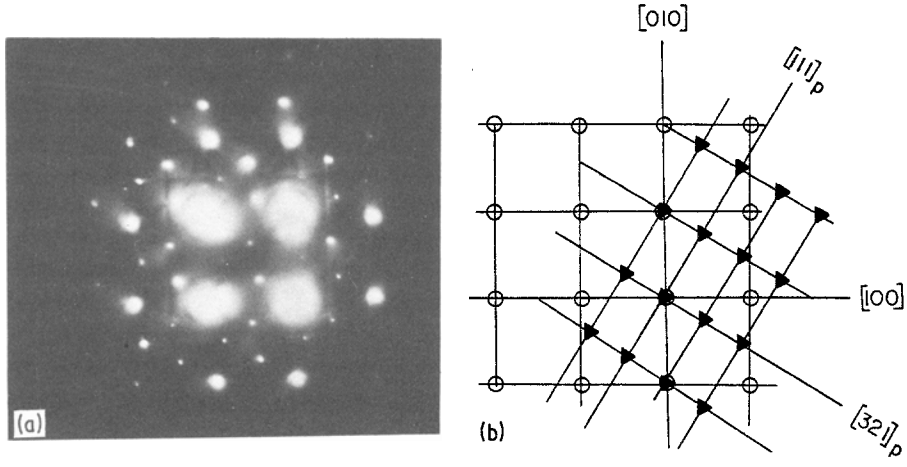

Figure 6 Selected-area diffraction pattern of a Ti_2C platelet in reaction-hot-pressed TiC.

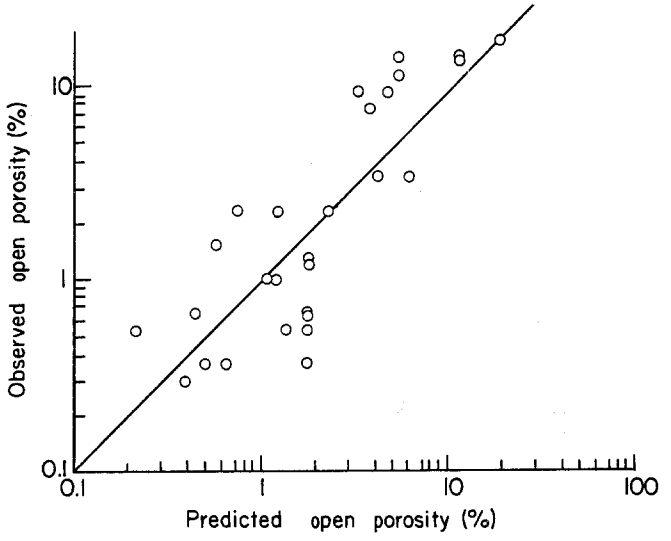

Figure 7 Observed open porosity against the values calculated from Equation 1c. The line indicates equality of observed and predicted values.

Examination of the residuals from the regression analysis indicates that there is some variability in the data which is not accounted for by the present model. The fit of this model to the hot-pressing data can be evaluated visually from Fig. 7 in which the experimental values of P are plotted against those predicted by Equation 1c.

5.2. Grain growth

In an earlier paper [3], the grain growth during sintering of titanium–titanium carbide compacts was described by a model adapted from Kuczysnki [7]. We will examine the applicability of Kuczysnki's grain-growth model to the data of the present hot-pressing study. The equation of interest from Kuczysnki describes the grain size, a, as a function of time, t, initial porosity, P, and starting grain-size, a_0:

$$a^n - a_0^n = \left[\frac{K_0^3 V_0 g^2}{P_0^{1-x}}\right]^{s-1/2x} \frac{nK_0\phi\alpha t}{P_0^s} \qquad (2)$$

where V_0 is the average pore volume at $t = 0$; ϕ is the probability of a pore having the proper neighbourhood for shrinkage; K_0 comes from Zener's relationship, $a = K_0 r/P$, where r is the average pore size; $\alpha = 8\pi\gamma\Omega d/[kT]$ where γ is the boundary energy, Ω is the atomic volume, and D is the diffusion coefficient for the process(es) which contribute to sintering; g_0 is a geometric factor relating the average pore volume, V_0, to the average pore radius.

Kuczysnki notes that Equation 2 is often observed to reduce to

$$a^3 - a_0^3 = (1 + x)K_0\phi\alpha t/P_0. \qquad (2a)$$

As noted previously [3], V_0, γ, and P_0 are functions of composition. In the case of hot pressing, the initial porosity (i.e. the porosity at the onset of grain growth) is a function of the applied pressure. Equation 1c describes the dependence of porosity on time and applied pressure. The small influence of time on the final density of hot-pressed samples is also evident in Equation 1c where P is shown to vary as $t^{0.1}$. Subsequent hot-pressing experiments in which the ram positions have been monitored indicate that most of the densification takes place in a matter of a few minutes after pressure is applied. The effective initial porosity for grain growth during hot pressing is, therefore, approximately equal to the final porosity and is a power-law function of the applied pressure. If these features are combined, the following equation can be considered for grain growth during hot pressing of titanium–titanium carbide compacts:

$$a^n - a_0^n = ADt\sigma^p C^q t/T. \qquad (2b)$$

Equation 2b was applied to the hot-pressing data by taking the logarithm of both sides and calculating the values of the exponents by a least-squares fit to the data. The value of a_0 was taken to be 14.3 μm on the basis of the previous sintering data [3]. As was observed with the sintering data, a value of $n = 3$ in Equation 2 gives the best fit. As a result of the regression analysis, the reactive hot pressing of titanium–titanium carbide mixtures is described by

$$(a^3 - a_0^3) = 1.5 \times 10^{-6}\ \mathrm{cm^3\ sec^{-1}} \times \exp\left[-230\ \mathrm{kJ}/RT\right] C^{-12}\sigma^{0.61} t^{0.46} \qquad (2c)$$

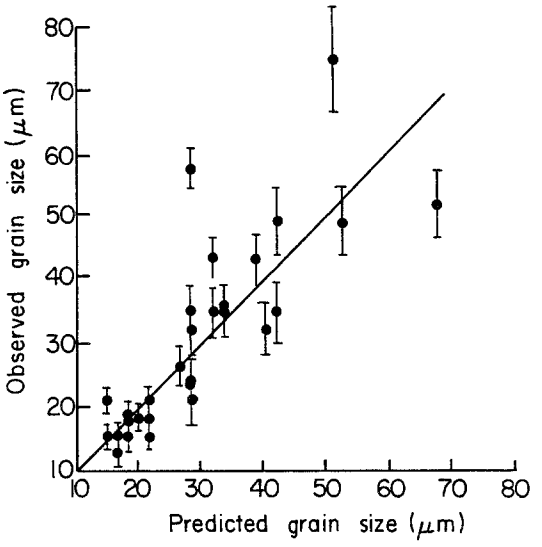

Figure 8 Observed grain size against the values calculated from Equation 2d. The line represents equality of observed and predicted values.

with $R^2 = 70.4\%$, adjusted for degrees of freedom. The fit of this model to the experimental data can be judged visually from Fig. 8 which is a plot of the measured values of grain size against those predicted by Equation 2c.

6. Discussion

The activation energy for grain growth during hot pressing, $230\,kJ\,M^{-1}$, is in good agreement with observed activation energy for the grain growth during reactive sintering, $260\,kJ\,M^{-1}$ [3]. Even though the titanium metal is observed to disappear rapidly, grain growth is strongly effected by composition. This correlation between grain growth and composition is due in large part to the marked decrease in porosity as a function of composition discussed for reactive sintering [3]. In addition, for the hot-pressed samples, there is a small effect of composition on the grain size among samples whose relative density is greater than 95%, with higher titanium contents leading to larger grain sizes. An increase in grain boundary energy or mobility with decreasing carbon–metal ratio may account for this grain-growth behaviour.

In the titanium–titanium carbide system the creep of the ductile titanium metal appears to play a large role in densification. The importance of the ductile behaviour of titanium metal is supported by the observation that high densities are obtained by hot-pressing mixtures of titanium with titanium carbide under conditions which yield only 85% dense samples from metal-free TiC powders. The activation energy for hot pressing, $11.7\,kJ\,M^{-1}$, agrees well with the activation energy for self-diffusion of titanium, $130\,kJ\,M^{-1}$ [11]. The activation energies for creep in metals, including titanium, at temperatures above half their melting point are observed to be in good agreement with activation energies for self diffusion [12]. Therefore, the activation energy for densification provides further confirmation of the role of the ductile behaviour of titanium in hot pressing.

The limited densification during reactive sintering was attributed previously to the rapid formation of a solid carbide skeleton [3]. The pressure applied during hot pressing may serve to break or inhibit the formation of some of the necks between carbide grains, thereby allowing the grains to move past each other as the titanium metal deforms.

The fit of this creep model, Equation 1b, to the open porosity data is limited by the formation of closed porosity and by the relatively poor control of the heating rate and the point at which pressure was initially applied. Uncertainties in heating rate and application of pressure introduce nonrandom sources of error. As a result, the time and temperature of the onset of pressing have a greater effect on final density at high temperatures and low pressures, where a rigid carbide skeleton might form most readily, than at low temperatures and high pressures.

Acknowledgements

The reaction hot-pressed samples were prepared at Corning Glass Works with the help of Mr Harry Watkins. Mr E. Harvey Barnett assisted in the design and analysis of the experiments. The transmission electron microscope was made available through the Central Facility for Electron Microscopy in the Materials Science Centre at Cornell University. This work is supported by the Department of Energy under grant No. DE-AC02-77ER04441 and by Corning Glass Works.

References

1. L. E. TOTH, "Refractory Materials" Vol. 6 (Academic, New York, 1971) p. 3.
2. E. K. STORMS, "Refractory Materials" Vol. 2 (Academic, New York, 1967) p. 1.
3. C. J. QUINN and D. L. KOHLSTEDT, *J. Mater. Sci.* 19 (1984) 1229.
4. "Metals Handbook", Vol. 1, edited by Taylor Lyman

(American Society for Metals, 1961).
5. F. KEIHN and R. KEBLER, *J. Less Common Metals* 6 (1967) 484.
6. G. E. P. BOX and D. W. BEHNKEN, *Technometrics* 2 (1960) 455.
7. G. C. KUCZYNSKI, in "Materials Science Research" Vol. 6, edited by G. C. Kuczynski (Plenum, New York, 1972) p. 217.
8. R. SPRIGGS and B. DUTTA, in "Materials Science Research" Vol. 6, edited by G. C. Kuczysnki (Plenum, New York, 1972) p. 417.
9. R. C. ROSSI and R. M. FULRATH, *J. Am. Ceram. Soc.* 48 (1965) 558.
10. C. J. QUINN and D. L. KOHLSTEDT, *J. Amer. Ceram. Soc.* (1984) submitted.
11. J. MURDOCK, T. LUNDY and E. STANSBURY, *Acta Metall.* 12 (1964) 1033.
12. F. McCLINTOCK and A. ARGON, "Mechanical Behavior of Materials" (Addison Wesley, Reading, Mass., 1966).

Received 22 June
and accepted 26 July 1983